BeBeC-2014-07

APPLICATION OF COMPRESSIVE SENSING BASED BEAMFORMING IN AEROACOUSTIC EXPERIMENT

Qingkai Wei[1], Bao Chen[2] and Xun Huang[1,3]
[1] Department of Aeronautics and Astronautics, College of Engineering, Peking University. 100871, Beijing, China.
[2] Aerodynamics Research Institut, Aviation Industry Corporation of China, Harbin, China.
[3] Airbus Noise Technology Centre, University of Southampton, Southampton, UK.

ABSTRACT

Compressive sensing (CS) is a newly emerging method in information technology that could reduce sampling efforts extensively by conducting L_1 optimization. In this work, CS is extended to array beamforming applications and two algorithms (CSB-I and CSB-II) are presented with the assumption of spatially sparse and incoherent sound sources. The two algorithms are examined using both simulation and aeroacoustic experiments. The simulation case clearly shows that the CSB-I algorithm is quite sensitive to the sensing noise. The CSB-II algorithm, on the other hand, is more robust to noisy measurements. In addition, aeroacoustic tests of an airplane model demonstrate the good performance in terms of resolution and sidelobe rejection of CSB-II algorithm.

1 INTRODUCTION

Compressive sensing [2, 4–6, 15], a new signal processing strategy from the field of information technology, reduces sampling efforts extensively by conducting L_1 optimization. This paper will apply this idea to beamforming techniques [17] that visualize signal of interest as measured by a sensor array. Potential applications can be found in acoustics [1, 7, 10, 13, 14, 18].

Recently, some compressive sensing based beamforming methods have been developed for direction-of-arrival estimation problem [8, 12]. The first paper demonstrated in numerical simulations that only a few samples are required compared with conventional beamforming. Compressive sensing beamforming was also applied to undersea data, manipulating the sensing matrix to maintain a stable calculation [8]. Most works in the literature use uniformly linear array [8, 12] and are examined only by simulation data. Aeroacoustic testing, on the other hand, uses a

different array layout. Aeroacoustic experiments performed in wind tunnel and anechoic chamber jet facility usually contain strong background noise at broadband frequencies. These issues from the specific application impose challenges to compressive sensing based beamforming.

This article will present a novel compressive sensing beamforming method and apply it to an aeroacoustic problem. It was verified using both simulated data with various signal-to-noise ratios (SNR) and measured aeroacoustic test data. The rest of the paper is organized as follows. In Section II, this algorithm is briefly introduced. Then, in Section III, validation results with both simulation and acoustic experiment are presented and discussed. Finally, the work is summarised in Section VI.

2 COMPRESSIVE SENSING BASED BEAMFORMING

2.1 Wave model

Given a sensory array with M microphones, the output $\mathbf{y}(t)$ denotes time domain measurements, $\mathbf{y} = (y_1 \dots y_i \dots y_M)^T \in \Re^{M\times 1}$ and $(\cdot)^T$ stands for transpose. For a single signal of interest $x(t) \in \Re^1$ in a free propagation space, using the associated Green's function, we can have

$$\mathbf{y}(t) = \frac{1}{4\pi\mathbf{r}} x(t-\tau), \tau = \frac{\mathbf{r}}{C}, \tag{1}$$

where C is the propagation speed; $\mathbf{r} \in \Re^{M\times 1}$ are the distances between $x(t)$ and sensors; and τ is the related sound propagation time delay.

For practical applications, beamforming is generally conducted in the frequency domain. The frequency domain version of Eq. (1) is:

$$\mathbf{Y}(j\omega) = \frac{1}{4\pi\mathbf{r}} X(j\omega) e^{-j\omega\tau} = \mathbf{G}_v(\mathbf{r}, j\omega) X(j\omega), \tag{2}$$

where $j = \sqrt{-1}$; $\mathbf{G}_v \in \mathfrak{C}^{M\times 1}$ is the associated steering vector; ω is angular frequency; $(j\omega)$ and $(\mathbf{r}, j\omega)$ are omitted in the following for brevity; $\mathbf{Y}$ and X are in the frequency domain. For simplicity, we can write Eq. (2) as $\mathbf{Y} = \mathbf{G}_v X$. The subscript $(\cdot)_v$ suggests that $\mathbf{G}_v$ is a vector.

The situation becomes more complicated for multiple signals of interest plus measurement noise. For clarity, the array output is represented in the scalar form,

$$\begin{bmatrix} Y_1 \\ \vdots \\ Y_i \\ \vdots \\ Y_M \end{bmatrix} = \begin{bmatrix} G_{11} & \dots & G_{1k} & \dots & G_{1N} \\ & & \vdots & & \\ G_{i1} & \dots & G_{ik} & \dots & G_{iN} \\ & & \vdots & & \\ G_{M1} & \dots & G_{Mk} & \dots & G_{MN} \end{bmatrix} \begin{bmatrix} X_1 \\ \vdots \\ X_k \\ \vdots \\ X_N \end{bmatrix} + \begin{bmatrix} N_1 \\ \vdots \\ N_i \\ \vdots \\ N_M \end{bmatrix}, \tag{3}$$

where G_{ik} is the steering vector between the ith sensor and the kth signal of interest; $Y_i(j\omega)$ is the ith sensory measurements; $X_k(j\omega)$ is the kth signal of interest; and $N_i(j\omega)$ is the collective measurement noise of the ith sensor. Potential noise sources include background interference

and electronic noise during data acquisition. For brevity, Eq. (3) can be written as

$$\mathbf{Y} = \mathbf{G}_{m_l}\mathbf{X} + \mathbf{N}, \tag{4}$$

where $\mathbf{G}_{m_l} \in \Re^{M\times N}$ is the associated matrix of steering vectors; and $\mathbf{X} \in \mathfrak{C}^{N\times 1}$ and $\mathbf{N} \in \mathfrak{C}^{M\times 1}$. Generally, it is assumed that $\mathbf{SX}$ and $\mathbf{N}$ are of zero-mean and statistically independent. In this work, we define the SNR of the kth sensor in decibels, as the following,

$$\mathrm{SNR}_{\mathrm{dB}} = 10\log_{10}\left(\frac{|\sum_{i=1}^{N} G_{ik}S_i|^2}{|N_i|^2}\right), \tag{5}$$

where the variables are the same as those in Eq. (3).

2.2 Compressive sensing

Candes *et al.* [5] proposed that a perfect reconstruction of a discrete-time signal $\sigma \in \mathscr{C}^N$ using sub-Shannon sampling rates is possible, as long as σ is *sparse* in some Hilbert basis $\psi \in \mathscr{C}^{N\times N}$, that is, $\sigma = \psi\alpha, \alpha \in \mathscr{C}^N$. The so-called *sparsity* means that the number of nonzero entries in α is pretty small, i.e. $||\alpha||_0 \ll N$.

According to compressive sensing theory, we can perform a small number of measurements to collect $\mathbf{y} = \phi\sigma$, where $\mathbf{y} \in \mathscr{C}^K$ and the sensing matrix $\phi \in \mathscr{C}^{K\times N}$, in the form of underdetermined linear equations. The sparse signal can then be reconstructed from those K projections by solving an L_1 regularization optimization [5],

$$\arg\min ||\hat{\alpha}||_1, \text{subject to } \phi\psi\hat{\alpha} = y_i, i = 1,...,K, \tag{6}$$

where $\hat{(\cdot)}$ represents the recovered estimation.

For those measurements polluted by some noise, a closely related programming with an error constraint should be adopted, as the following

$$\arg\min ||\hat{\alpha}||_1, \text{subject to } ||\mathbf{y} - \phi\psi\hat{\alpha}||_2 \leq \delta, \delta > 0. \tag{7}$$

In this work, δ is empirically chosen according to the corresponding SNR.

The above programming can be resolved using any available convex optimization tools, such as CVX [3]. Once $\hat{\alpha}$ is achieved, the original signal σ can be straightforwardly recovered as $\psi\hat{\alpha}$. The reconstruction error is negligible with a high probability if

$$K > C_k \cdot M \cdot \log(N/M), \tag{8}$$

where C_k is a universal constant that directly determines the accuracy of the optimization outcomes. A small C_k, such as 2, could work if the mutual coherence between ϕ and ψ is small. Random projections for ϕ is thus recommended in the literature for their general incoherence with respect to most fixed transformation basis ψ.

2.3 Compressive sensing based beamforming

To the best of our knowledge, beamforming work based on compressive sensing is rarely applied to practical applications as yet. Because the only way to validate an algorithm is to apply it for practical applications, the main contribution of this work fills the gap, developing compressive sensing based beamforming algorithms for one of aeroacoustic applications.

In this work, signals of interest are presumably regarded as spatially sparse. The same assumption has been adopted in the literature [11] for bearing estimation. Then, by checking with Eq. (7) and Eq. (4), we can simply propose a straightforward algorithm of compressive sensing based beamforming,

$$\arg\min ||\hat{\mathbf{S}}||_1, \text{subject to } ||\mathbf{Y} - \mathbf{G}_{m_I}\hat{\mathbf{S}}||_2 \leq \delta, \delta > 0, \tag{9}$$

where δ is empirically assigned according to the corresponding SNR, and $\delta = 0$ if the measurements are free of noise (i.e., SNR $= \infty$). In addition, the beamforming results are generally represented by signal power. Then, the estimated signal power is

$$\mathbf{P}_{CSB-I} = ||\hat{\mathbf{S}}||_2. \tag{10}$$

For convenience, this compressive sensing beamforming is denoted by CSB-I in the following.

In this work, we developed a new compressive sensing beamforming algorithm based on so-called cross spectrum matrix (also known as covariance matrix or cross-spectral density matrix). The definition is

$$\mathbf{R} = \mathrm{E}\{\mathbf{Y}\mathbf{Y}^*\}, \tag{11}$$

which can be approximated by

$$\hat{\mathbf{R}} \approx \frac{1}{K}\sum_{k=1}^{K}\mathbf{Y}\mathbf{Y}^*, \tag{12}$$

where K is the number of sampling blocks. For statistical confidence, the associated sampling duration should be much larger than the the period of signal of interest.

The associated algorithm is called CSB-II throughout this article. Its derivation is as the following. From Eq. (3), we have

$$\mathbf{R}_V = \begin{bmatrix} G_{11}G_{11}^* & G_{12}G_{12}^* & \cdots & G_{1N}G_{1N}^* \\ G_{11}G_{21}^* & G_{12}G_{22}^* & \cdots & G_{1N}G_{2N}^* \\ & & \vdots & \\ G_{M1}G_{M1}^* & G_{M2}G_{M2}^* & \cdots & G_{MN}G_{MN}^* \end{bmatrix}\mathbf{P} + \mathbf{Q} = \mathbf{G}_{m_{II}}\mathbf{P} + \mathbf{Q}, \tag{13}$$

where $\mathbf{R}_V = (\mathrm{E}[Y_1Y_1^*], \mathrm{E}[Y_1Y_2^*], \cdots, \mathrm{E}[Y_MY_M^*])^T \in \mathfrak{C}^{M^2\times N}$ is a vector that can be approximately achieved by reshaping $\hat{\mathbf{R}}$ [Eq. (12)]; the symbol of $(\cdot)^*$ denotes the conjugate transpose; $\mathbf{P} = [S_1S_1^*, S_2S_2^*, \cdots, S_NS_N^*]^T \in \mathfrak{R}^{N\times 1}$, where S_i and S_k $(i \neq k)$ are incoherent; and $\mathbf{Q}$ is the vertical vector form of $\mathrm{E}[\mathbf{N}\mathbf{N}^*] \in \mathfrak{C}^{M^2\times 1}$. Then, the proposed CSB-II algorithm works by solving

$$\arg\min ||\hat{\mathbf{P}}||_1, \text{subject to } \hat{\mathbf{P}} > 0, ||\hat{\mathbf{R}}_V - \mathbf{G}_{m_{II}}\hat{\mathbf{P}}||_2 \leq \delta, \delta > 0. \tag{14}$$

As a result, the estimated signal power is

$$\mathbf{P}_{CSB-II} = \hat{\mathbf{P}}. \tag{15}$$

In summary, both the algorithms developed in this work are started by,
Step 0: Collect measurements and obtain $\mathbf{Y}$ by performing Fourier transform.
Then, the CSB-I algorithm is conducted as the following,
Step 1: Prepare $\mathbf{G}_{m_I}$ using Eqs. (2)–(4).
Step 2: Calculate the CSB-I beamforming with Eqs. (9)–(10). Done.
On the other hand, the steps of the CSB-II algorithm include
Step 1: Prepare $\mathbf{G}_{m_{II}}$ using Eq. (13).
Step 2: Prepare $\mathbf{R}_V$ by reshaping $\hat{\mathbf{R}}$ that is calculated with Eq. (12).
Step 3: Perform l_1-minimization and achieve the CSB-II beamforming results, using Eqs. (14)–(15). Done.

3 RESULTS AND DISCUSSION

A simulation case was conducted firstly to quantity the performance of the proposed algorithms. In the simulation, we assume free space propagation for a monopole 5 kHz sources that locates at the origin, 1 m away from the array. For this simple case, we just use 10 microphones, which are randomly chosen in the array, to yield the beamforming results. In addition to this sound signal, we assume that each sensor also perceive a white noise, which could come from background noise or electronic noise.

Various SNR levels, from ∞ to -10 dB, have been tested. According to Eq. (5), SNR $= \infty$ suggests a negligible noise; SNR $= 0$ dB suggests that the power from the monopole signal equals the power from the background noise; and SNR $= -10$ dB suggests that the power of the background noise is ten times greater than the power of the monopole signal.

Figures 1(a-b) show the normalized beamforming results using the CSB-I algorithm. The dynamic range of the CSB-I results is more than 100 dB and those data smaller than -100 dB is cut off for clarity of the figures. In Fig. 1(a), the simulated measurements are free of background noise (i.e., SNR $= \infty$). It can be seen that the CSB-I algorithm perfectly capture the desired signal with very fine resolution and nice sidelobe rejection. However, as the value of SNR decreases, we found that the CSB-I algorithm fails to output reasonable results. For example, when SNR $= -10$ dB, Fig. 1(b) shows that false signal sources scatter on the entire imaging domain. In contrast, Fig. 1(c) shows that the CSB-II algorithm is still able to capture the mainlobe as well as maintain a good sidelobe rejection. The dynamic range is however diminished to 60 dB that is still quite satisfactory.

Figure 1(d) examines the x-axial performance on the dashed line, which has been shown in Fig. 1(b). In comparing CSB-I and CSB-II algorithms with conventional beamforming (CB), the following expression is used,

$$\sigma_{CB} = \mathbf{W}^* \hat{\mathbf{R}} \mathbf{W}, \mathbf{W} = (\mathbf{G}_v^* \mathbf{G}_v)^{-1} \mathbf{G}_v. \tag{16}$$

The above CB algorithm is narrowband and only for a single gridpoint. We have to scan each gridpoint of the imaging plane using this algorithm to yield the desired images at frequency ranges of interest. It can be seen that the CB algorithm produces a very broad mainlobe. The

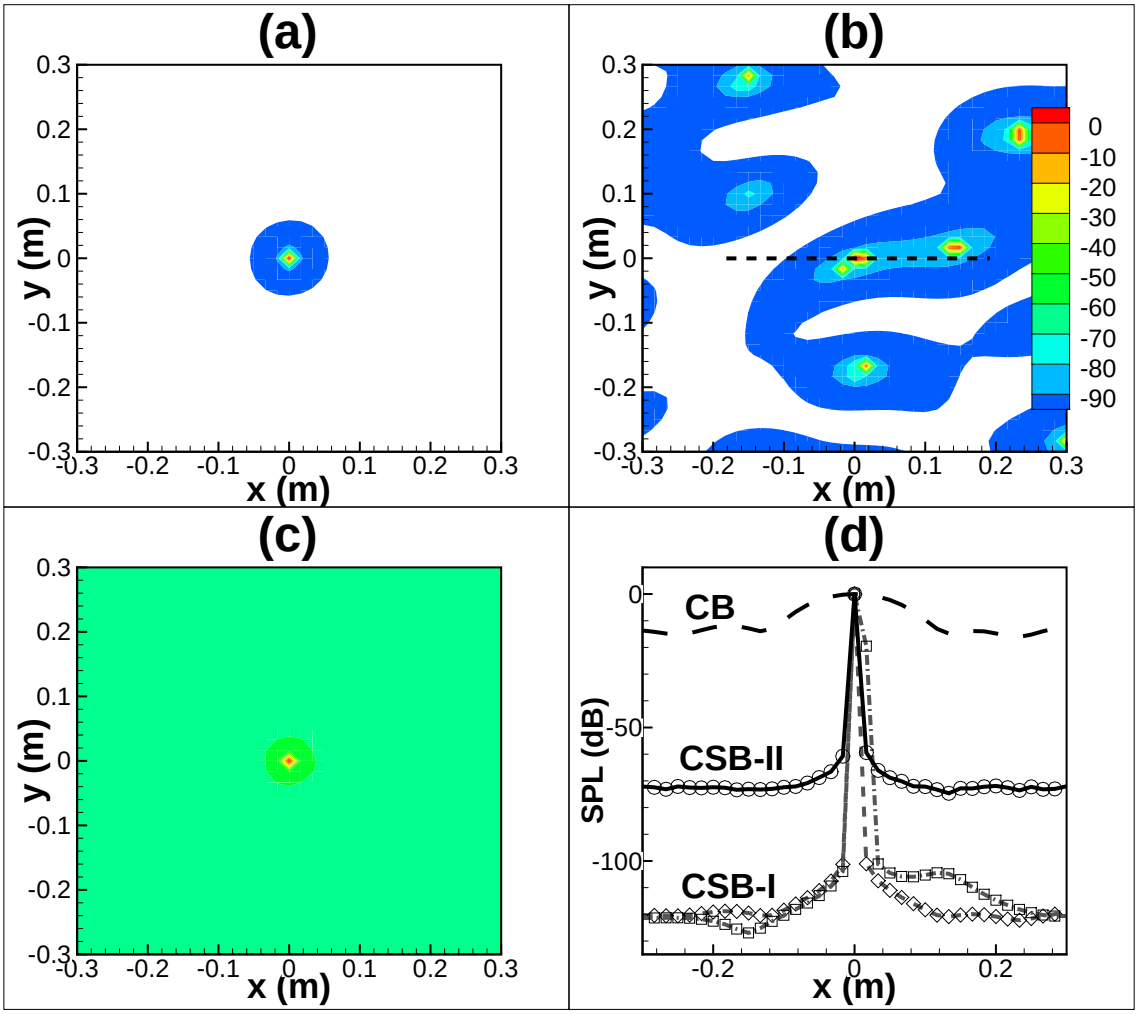

Figure 1: Beamforming results of the monopole case at 5 kHz, where: (a) SNR $= \infty$*, CSB-I; (b)* SNR $= -10\,dB$*, CSB-I; (c)* SNR $= -10\,dB$*, CSB-II; and (d) the x-axial only performance, (−−) the CB result for* SNR $= -10\,dB$*, (⋄) the CSB-I result for* SNR $= \infty$*, (□) the CSB-I result for* SNR $= -10\,dB$*, and (○) the CSB-II result for* SNR $= -10\,dB$*. The contour levels in (a-c) are set between* $-100\,dB$ *and* $0\,dB$*. The levels below* $-100\,dB$ *are cut off.*

associated dynamic range is slightly over 10 dB. Then, Fig. 1(d) clearly identify the distinctive performance of CSB algorithms, in terms of the resolution and dynamic range. In addition, the CSB-II algorithm can suppress detrimental interference of noisy measurements to some extent. In this very simple case with an idealized monopole source, the CSB-II algorithm fails to produce correct results if SNR is smaller than −15 dB. On the other hand, the CSB-I algorithm fails quickly when SNR is just 0 dB. As a result, only the CSB-II algorithm is applied in the following practical test.

Test data achieved in our previous experiments is used to demonstrate compressive sensing

beamforming methods. The experiments were conducted in lined wall closed-section wind tunnel at Aerodynamics Research Institute, AVIC. The maximum flow speed in the test section could reach 130 m/s and the associated Reynolds number is 8.5×10^6. The test section of the wind tunnel is 4.5 m $\times$3.5 m $\times$11 m (width $\times$ height $\times$ length).

A 1/12 scaled model of the commercial transport aircraft, Modern Ark 60 (MA-60), manufactured from aluminum is tested to evaluate the new aeroacoustic treatments of the wind tunnel with lined wall (see Fig. 2). The angle of attack, α, of the model can be modified during tests. Various aerodynamic setups have been tested in this experiment and the evaluation of the aeroacoustic treatments of the closed-section wind tunnel is presented in another paper. In this paper, the condition, the angle of attack α is 6 deg when the wind speed is 40 m/s, is considered in the validation of CSB-II algorithm.

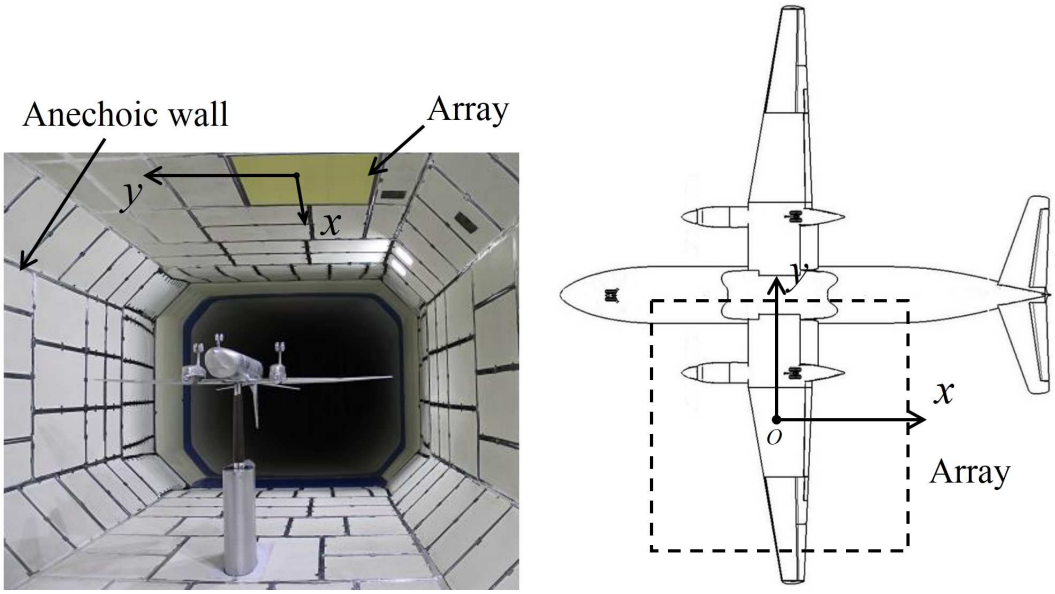

(a) (b)

Figure 2: A 1/12 scaled model of the commercial transport aircraft (MA-60) was installed in the lined test section of a closed wind tunnel, where (a) the photo taken in the test section, and (b) the ceiling view of the experimental setup.

An array consisting of 110 channels of Brüel and Kjær 4954 microphones is mounted on the ceiling of the test section (see Fig. 2(a)) to acoustically 'visualize' flow-induced noise sources. The layout of the microphones is a multi-arm spiral line, which is *de facto* adopted in acoustic tests. The microphones are recessed by almost 2 mm beneath the Kevlar cloth to suppress boundary layer interference [9, 16]. The frequency response of each microphone is carefully calibrated to maintain perfect array performance.

Most compressive sensing works are validated using simulation results. Very few beamforming results from compressive sensing can be found in the literature for practical experimental data. It should be interesting to apply the proposed method to practical aeroacoustic test data. The CSB-II result is compared to that obtained with the CB algorithm. Figure 3 shows results at 4 kHz when the wind speed is 40 m/s. The contour levels are between -10 dB and 0 dB for

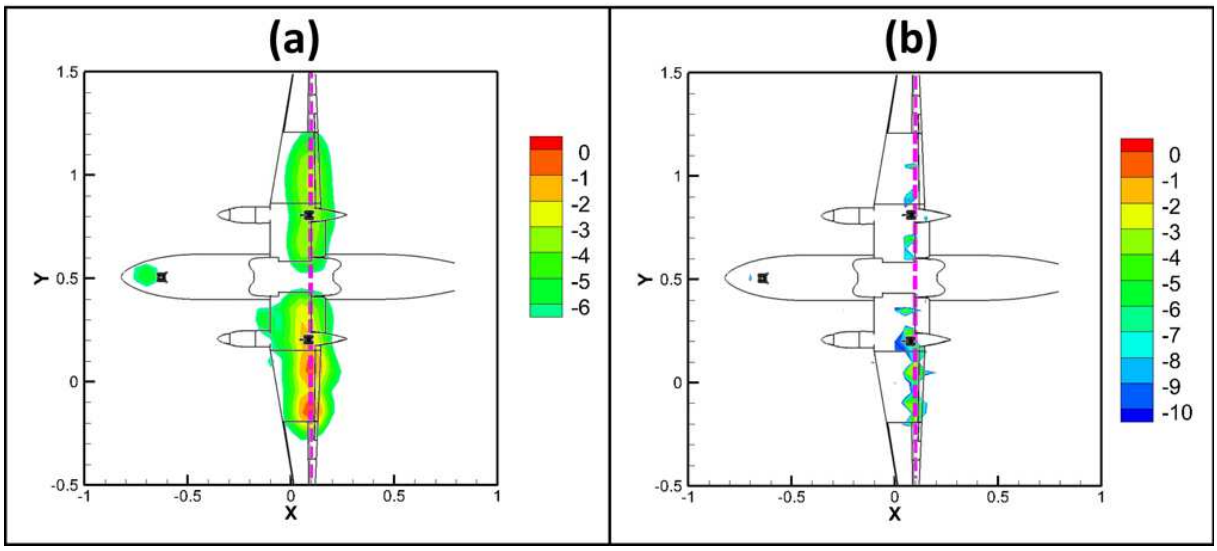

Figure 3: Acoustic images at 4 kHz, 40 m/s, (a) using conventional beamforming algorithm; (b) using CSB-II algorithm.

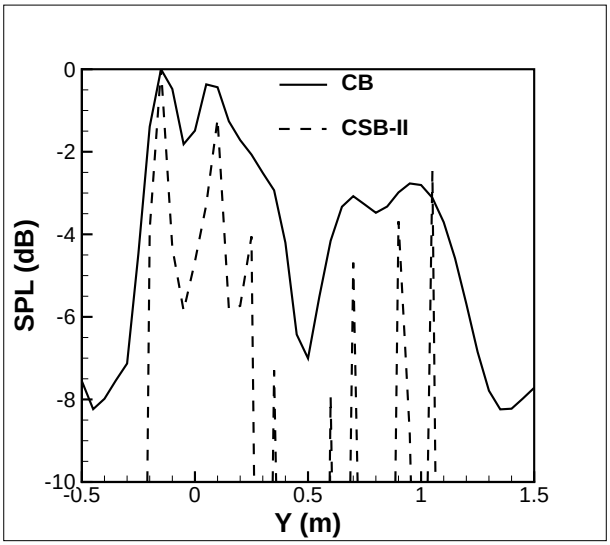

Figure 4: Comparison of SPL on the line shown in Fig. 3.

the CSB-II method, while for the CB method, the dynamic range could only reach 6 dB. It needs to be mentioned that, the SPL levels have been normalised with the maximum level in the scanning area. In addition, Figure 4 shows the SPL level on the line along the wing marked in Fig. 3.

Compared to the CB results, the CSB-II results have a better resolution (with narrow main-lobes) and smaller sidelobe levels. In short, the imaging quality is improved with the proposed

compressive sensing based beamforming method.

4 SUMMARY

Compressive sensing is the newly emerging method in information technology that could significantly impact acoustic research and applications. In this article, we firstly introduced the fundamentals of compressive sensing theory. After that, we implemented two different compressive sensing based beamforming algorithms (CSB-I and CSB-II). Both algorithms are proposed for those presumably spatially sparse and incoherent signals.

The two algorithms are examined using a simple simulation case and a practical aeroacoustic test case. The simulation case clearly shows that the CSB-I algorithm is quite sensitive to the sensing noise. The CSB-II algorithm, on the other hand, is more robust to noisy measurements. The results by CSB-II at SNR $= -10$ dB are reasonable with good resolution and sidelobe rejection. Although the inherent reason is not discussed in this work, we believe it has connection with the so-called restricted isometry property [5]. Detailed analysis id beyond the scope of this paper.

The proposed method was then successfully evaluated and demonstrated in the numerical simulations. The sound source considered in the simulation case is an idealised monopole. Few results for practical experimental data can be found in the literature. This work develops compressive sensing based beamforming algorithms specifically for aeroacoustic tests and applies it to the practical data in an effort to fill this gap. The CSB-II algorithm is applied to experimental data acquired in a lined wall closed-section wind tunnel. The results suggest that the proposed CSB-II algorithm is robust to potential interference in practical tests, and can produce an acoustic image with a significant improvement of resolution.

5 ACKNOWLEDGMENTS

This research was supported by the NSF Grant of China (Grants Nos. 11172007 and 11322222) and AVIC Commercial Aircraft Engine Co., LTD.

References

[1] L. Bai and X. Huang. "Observer-based beamforming algorithm for acoustic array signal processing." *Journal of Acoustical Society of America*, 130(6), 3803–3811, 2011.

[2] R. G. Baraniuk. "More is less: Signal processing and the data deluge." *Science*, 331(11), 717–719, 2011.

[3] S. Boyd and L. Vandenberghe. *Convex Optimization*. Cambridge University Press New York, 2004.

[4] E. J. Candes. "Near-optimal signal recovery from random projections: Universal encoding strategies?" *IEEE Transaction on Information Theory*, 52(12), 5406–5425, 2006.

[5] E. J. Candes, J. Romberg, and T. Tao. "Robust uncertainty principles: Exact signal reconstruction from highly incomplete frequency information." *IEEE Transaction on Information Theory*, 52(2), 489–509, 2006.

[6] E. J. Candes and M. B. Wakin. "An introduction to compressive sampling." *IEEE Signal Processing Magzaine*, 25(2), 21–30, 2008.

[7] Y. T. Cho and M. J. Roan. "Adaptive near-field beamforming techniques for sound source imaging." *Journal of Acoustical Society of America*, 125(2), 944–957, 2009.

[8] G. F. Edelmann and C. F. Gaumond. "Beamforming using compressive sensing." *Journal of Acoustical Society of America*, 130(4), EL232–EL237, 2011.

[9] V. Fleury, L. Coste, R. Davy, A. Mignosi, C. Cariou, and J.-M. Prosper. "Optimization of microphone array wall mountings in closed-section wind tunnels." *AIAA Journal*, 50(11), 2325–2335, 2012.

[10] R. A. Gramann and J. W. Mocio. "Aeroacoustic measurements in wind tunnels using adaptive beamforming methods." *Journal of Acoustical Society of America*, 97(6), 3694–3701, 1995.

[11] A. C. Gurbuz, V. Cevher, and J. H. McClellan. "Bearing estimation via spatial sparsity using compressive sensing." *IEEE Transactions on Aerospace and Electronic Systems*, 48(2), 1358–1369, 2012.

[12] A. C. Gurbuz, J. H. McClellan, and V. Cevher. "A compressive beamforming method.", 2008. IEEE Acoustics, Speech and Signal Processing.

[13] X. Huang, L. Bai, I. Vinogradov, and E. Peers. "Adaptive beamforming for array signal processing in aeroacoustic measurements." *Journal of Acoustical Society of America*, 131(3), 2152–2161, 2012.

[14] Y. Liu, A. R. Quayle, A. P. Dowling, and P. Sijtsma. "Beamforming correction for dipole measurement using two-dimensional microphone arrays." *Journal of Acoustical Society of America*, 124(1), 182–191, 2008.

[15] J. Romberg. "Imaging via compressive sampling." *IEEE Signal Processing Magzaine*, 25(2), 14–20, 2008.

[16] H.-C. Shin, W. Graham, P. Sijtsma, C. Andreou, and A. C. Faszer. "Implementation of a phased microphone array in a closed-section wind tunnel." *AIAA Journal*, 45(12), 2897–2909, 2007.

[17] B. D. Van Veen and K. M. Buckley. "Beamforming: A versatile approach to spatial filtering." *IEEE ASSP Magazine*, 5(2), 4–24, 1988.

[18] T. Yardibi, J. Li, P. Stoica, and L. N. Cattafesta. "Sparsity constrained deconvolution approaches for acoustic source mapping." *Journal of Acoustical Society of America*, 123(5), 2631–2642, 2008.